Changes in Single K^+ Channel Behavior Induced by a Lipid Phase Transition

Heiko M. Seeger,[†] Laura Aldrovandi,[†] Andrea Alessandrini,[†‡] and Paolo Facci[†*]
[†]Centro S3, CNR-Istituto Nanoscienze, Modena, Italy; and [‡]Department of Physics, University of Modena and Reggio Emilia, Modena, Italy

ABSTRACT We show that the activity of an ion channel is correlated with the phase state of the lipid bilayer hosting the channel. By measuring unitary conductance, dwell times, and open probability of the K^+ channel KcsA as a function of temperature in lipid bilayers composed of POPE and POPG in different relative proportions, we obtain that all those properties show a trend inversion when the bilayer is in the transition region between the liquid-disordered and the solid-ordered phase. These data suggest that the physical properties of the lipid bilayer influence ion channel activity likely via a fine-tuning of its conformations. In a more general interpretative framework, we suggest that other parameters such as pH, ionic strength, and the action of amphiphilic drugs can affect the physical behavior of the lipid bilayer in a fashion similar to temperature changes resulting in functional changes of transmembrane proteins.

INTRODUCTION

The biological membrane configures a tremendously complicated ensemble which controls all the communications between the inner and outer regions of cells and organelles. It is mainly composed of lipids and proteins which cooperate to assure biological functions. In recent years, it has become increasingly evident that the lipid bilayer not only provides a medium for transmembrane protein folding and diffusion, but with its dynamic heterogeneity, participates actively in the fine control of protein functionality (1,2).

Exploiting model systems of increasing complexity we are gaining knowledge on the unifying physical principles underlying lipid/transmembrane protein interactions (3). The mutual interplay between transmembrane proteins and lipids composing the bilayer can be the result of either specific interactions or nonspecific collective bilayer properties (4). In the latter case, the lipid bilayer is considered as a continuum medium, characterized by certain mechanical properties (5).

A transmembrane protein which accomplishes its function by a conformational change involving the lipid/protein interface will be influenced, as far as its functionality is concerned, by the lipid bilayer's properties (6,7). These include bilayer thickness, compressibility, lateral pressure profile, and surface charge. Many of these properties change abruptly during the bilayer's main phase transition which represents the switching of the bilayer organization from the solid-ordered phase, characterized by lateral and molecular order, to the liquid-disordered phase in which both levels of order decrease. For example, fluctuations in area, enthalpy, and volume are enhanced and slowed down in the phase transition region, leading to a more compressible bilayer (8–11).

It has already been reported that the Arrhenius plots of the functional activity of many membrane-bound enzymes or transport membrane proteins show breaks which are considered hallmarks of lipid phase transitions (12). From a biological point of view, the proximity of a system to a phase transition assures a convenient and very efficient way to control biological functions with a very small variation in the environmental parameters. In fact, the transition can be induced by a change in temperature or in other physical-chemical parameters. This condition has been recently considered important in many biologically relevant situations, including dynamic heterogeneity in lipid bilayers and the cytoskeleton (13,14).

Ion channels represent important paradigmatic examples of transmembrane proteins. The effect of temperature on the ion channel activity, including the unitary conductance and the gating properties, has been studied in the past to characterize the energetic requirements involved in the permeation process (15–18). Many works have reported nonlinear Arrhenius plots of the channel activity both for the conductance and for rate constants (17,19,20). The discontinuity in the slope is usually interpreted as a strong indication of a phase transition, whereas a continuous change of the slope is expected in cases of a broad two-phase coexistence region. However, even if the observed behavior of a channel can be understood in terms of membrane thermodynamics, there is no direct experimental evidence connecting directly the channel functional behavior to the physical state of the membrane at the single molecule level.

Here we used the ion channel KcsA to study the effect of the lipid bilayer phase state on protein ion channel functionality. KcsA from *Streptomyces lividans* is a homotetrameric K^+ channel which can be gated by cytoplasmic pH changes (21–23). Its open probability increases at acidic pH with a half-transition pH of 4.2 for the wild-type channel (24). KcsA is the first K^+ channel whose structure has been solved by x-ray crystallography, shedding light on many of the structural properties of K^+ ion channels (25,26).

Submitted July 15, 2010, and accepted for publication October 22, 2010.

*Correspondence: p.facci@unimo.it

Editor: Eduardo Perozo.

0006-3495/10/12/3675/9 $2.00

doi: 10.1016/j.bpj.2010.10.042

Due to its well-known structure, KcsA has become the experimental model system of choice to study ion channel and transmembrane protein properties also in relation to protein/lipid interaction. Generally, one assumes that the transition to the open state involves a lateral area expansion of the channel in a deformation-resistant lipid bilayer (27,28). Thus, protein conformational variations are likely to be affected by the physical state of the membrane (27).

MATERIALS AND METHODS

Sample preparation

The lipids POPE (1-palmitoyl-2-oleoyl-*sn*-glycero-3-phosphoethanolamine) and POPG (1-palmitoyl-2-oleoyl-*sn*-glycero-3-[phospho-*rac*-(1-glycerol)] (sodium salt) were purchased from Avanti Polar Lipids (Alabaster, AL) and used without further purification. Stock solutions (in $CHCl_3$) were mixed to obtain the desired lipid molar ratios of 3:1, 1:1, and 0:1 (POPE/POPG). Then the chloroform was evaporated under a flow of nitrogen while heating the sample in a water bath at 50°C. Thereafter, the sample was kept under vacuum (10^{-2} mbar) for at least 4 h to remove residual chloroform molecules. Samples which were not immediately used were flushed with nitrogen and stored at −80°C. For the functional studies, we added 100 μL of chloroform to obtain a final concentration of 5 mg/mL before usage.

For protein reconstitution, the lipids were rehydrated in a buffer solution of 450 mM KCl, 25 mM HEPES at a pH of 7 to obtain a final lipid concentration of 10 mg/mL. The sample was stirred at ~30°C for 1 h. During this time, the sample was vortexed at least two times. For DSC measurements, we added 125 mM KCl, 25mM KOH, and 10 mM potassium dihydrogen citrate at pH values of 3, 4.5, and 6.5 to obtain a final lipid concentration of 10 mM. The sample was stirred at ~30°C for 1 h. During this time, the sample was vortexed at least twice.

KcsA expression, purification, and reconstitution

KcsA with an additional N-terminal hexahistidine sequence was expressed in BL21(DE3) cells grown in TB medium (23,29). Protein expression was induced by addition of 0.2 mg/L anhydrotetracycline (Acros Organics, Geel, Belgium). The expressed protein was extracted with 20 mM decylmaltoside and purified by Nickel affinity chromatography on a HisTrap FF crude column (Amersham Biosciences, GE Healthcare, Piscataway, NJ). The protein was eluted in 5 mM decylmaltoside, 25 mM KCl, 50 mM NaH_2PO_4, 32 mM NaOH, and 400 mM Imidazole, pH 7.0. Immediately after Nickel affinity purification, the protein was concentrated and reconstituted by dialysis into POPE/POPG 3:1 (molar/molar) lipid vesicles following the procedure described in Schmidt et al. (30) with a protein/lipid ratio (w/w) ranging from 0.001 to 0.005 (functional studies) or 0.1–0.5 (atomic force microscopy). The prepared proteo-liposomes were stored at −80°C until usage. We performed the functional studies in varying ratios of POPG and POPE. The KcsA channels used to perform the functional studies were always reconstituted in POPE/POPG 3:1 mixtures. It was shown before that the functional data depend solely on the lipid ratio used for the black lipid membrane formation and not on the lipid ratio, which in this case is always the same, of the proteo-liposomes used to incorporate KcsA in the black lipid membranes (BLMs) (31).

Single channel measurements

Vertical planar lipid bilayers were prepared over a round aperture with a diameter of 150–200 μm in a Teflon foil (25-μm thickness; DuPont, Wilmington, DE) separating two compartments (Montal-Muller method) (32). Before usage, the setup was cleaned with acetone, bidistilled water, and acetone and then it was dried under a nitrogen stream. After waiting 15 min, the round aperture was prepainted using a solution of *n*-pentane/*n*-hexadecane (10:1). After 15 min, the two compartments were filled with 1 mL of the desired buffer solution of 125 mM KCl, 25 mM KOH, 10 mM potassium dihydrogen citrate at pH 3 and pH 6.5 in the two compartments, respectively. Then we added two Ag/AgCl electrodes, which were embedded in agar-salt bridges (1.5% agar, 3 M KCl). The grounded electrode was inserted in the compartment with the buffer at pH 6.5 (*cis* side) and the input electrode was inserted to the one at pH 3 (*trans* side). Then we added 10–15 μL of the 5 mg/mL lipid in chloroform solution with the desired POPE/POPG molar ratios to both compartments. We waited for 15 min after which we raised the water levels above the aperture by adding another 1 mL of the respective buffer solutions to both compartments.

At first we obtained a capacity of ~0.2 $\mu F/cm^2$ resulting from the formation of a hexadecane layer. This layer could not be destroyed even by applying holding potentials above 500 mV. We destroyed this layer mechanically and controlled the quality of the Ag/AgCl electrodes by determining their offset voltage. Electrodes requiring an offset-voltage of >10 mV were discarded. We then prepared a lipid bilayer across the aperture. In general we obtained lipid bilayers with a specific capacity of ~0.4 to 0.8 $\mu F/cm^2$. Applying voltages between 300 mV and 500 mV resulted in the breaking of the lipid bilayer. We then thawed the proteo-liposomes and sonicated them in an ultrasonic bath for 30 s. Then we added 5 μL of proteo-liposome solution to the *trans* side (pH 3). For temperature-control of the planar bilayer setup, we used water circulation around the bilayer cell. The temperature was determined in a separate gauging measurement as a function of the heat bath temperature. The temperature was measured by a digital thermometer model No. 16 (Fluka, Buchs, Switzerland) equipped with a small K-thermocouple probe (Thermocoax, Stapelfeld, Germany). Temperature was changed at a rate of 5°C/h as done in the DSC experiments (see below).

During the recording of ion current traces temperature did not vary significantly (<0.1°C). The planar bilayers can be easily destroyed at relatively high holding potentials and become more and more sensitive in the phase transition regime where we had to limit the holding potentials between −100 mV and 100 mV. For data acquisition, we used an EPC 8 patch-clamp amplifier (Heka, Freiburg, Germany). The data were recorded using GePulse software (Pusch lab, CNR-Institute of Biophysics, Genova, Italy) at a rate of 10 kHz and they were subjected to a seven-pole Bessel filter at 1 kHz. Depending on the purpose of the measurement we recorded traces with a length of time ranging from 5 min to 20 min. Data were analyzed without further filtering using either Analysis software (Pusch lab) or QUB software (State University of New York at Buffalo, Buffalo, NY). Ion current histograms were fitted with Gaussian distributions. Single channel conductance and open probabilities are reported as mean ± SD on a base of four experiments.

It is to be stressed that it is impossible to assemble two systems which share the same physical properties due to difficulties inherent to the experimental setup (e.g., differences in lateral pressure of the leaflets and possible residual solvent). However, the differences in the temperature at which the trend inversion starts are within 0.5°C for the experiments performed on the same lipid mixture. For an analysis of the ion channel's kinetics, only sequences which showed the presence of one active channel were considered. Then, the ion current traces were idealized in noise-free open and closed transitions using the segmental k-means algorithm (33,34). The outcome was controlled visually. Dwell-time data were assembled in a logarithmic time axis on the abscissa and a square-root ordinate which was normalized for representation. The nonnormalized dwell-time histograms were fitted with exponential components.

Differential scanning calorimetry

Differential scanning calorimetry (DSC) measurements were performed with a VP-DSC from Microcal (Northampton, MA) using high feedback

mode at a scan rate of 5°C/h. Suspensions of POPE/POPG 3:1 or 1:1 in buffer solutions of 125 mM KCl, 25 mM KOH, 10 mM potassium dihydrogen citrate at pH values of 3, 4.5, and 6.5 at a lipid concentrations of 10 mg/mL were sonicated in an ultrasonic bath for 30 s to obtain small unilamellar vesicles before the measurements. Excess heat capacity profiles of the sample were directly measured in the calorimeter cell.

RESULTS

Thermodynamics of POPE/POPG membranes

In this study, we aimed at investigating the functional properties of an ion channel as a function of the lipid bilayer's physical state. This aspect required a detailed understanding of the physical properties of the lipid system under varying conditions. Thus, at first we performed DSC characterizations of small unilamellar vesicles composed by POPE/POPG 3:1 and 1:1 at different pH. Fig. 1 *a* displays the excess heat capacity profiles as a function of pH for a mixture of POPE/POPG 3:1 measured from high to low temperature. For all the displayed pH values, the melting transition regime lied between 14°C and 26°C and shifted to higher temperatures for more acidic pH. Fig. 1 *b* reports the transition midpoint temperature (T_m) versus pH for both the upscan (low temperature to high temperature) and the downscan (high temperature to low temperature) directions. It appeared that T_m depended linearly on pH. The melting transition showed hysteresis, so that the calorimetric profiles were shifted by ~1.5°C to lower temperatures when cooling the bilayer with respect to the heating scans.

We have also compared the phase transition regime of sonicated and nonsonicated liposomes of POPE/POPG 3:1. We have not found any appreciable difference between these systems. This investigation allowed us to establish that, for the lipid system at issue, the phase transition from liquid-disordered to solid-ordered phase occurs around room temperature (from 18° to 23°C). In the case of the pure POPG bilayer, the transition occurs at a temperature below

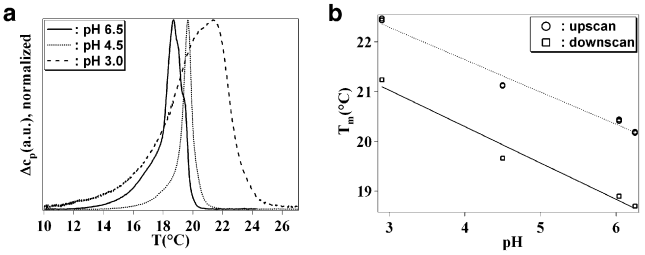

FIGURE 1 Thermodynamic characterization of the main phase transition behavior of POPE/POPG 3:1 bilayers. (*a*) DSC curves acquired starting from high to low temperatures are reported for POPE/POPG 3:1 at varying pH values. (*b*) Variation of the transition midpoint temperature of the POPE/POPG 3:1 bilayers as a function of pH. Both the temperatures obtained from the upscan and the downscan of the DSC measurements are given highlighting the hysteretic behavior. The markers (○, upscan; □, downscan) display the measured values, while the lines represent linear fits to the experimental data.

0°C at neutral pH (35). The phase transition in the presence of both POPE and POPG is characterized by a broad phase coexistence region where the liquid-disordered phase will be enriched in POPG and the solid-ordered phase will be enriched in POPE. The temperature at which the experiments on BLMs are performed is usually not reported in the literature. Thus, it is reasonable to assume that they are performed at room temperature. For the lipid mixture usually employed in the case of KcsA (POPE/POPG 3:1), the room temperature includes the phase transition region of the lipid bilayer.

Also in the case of POPE/POPG 1:1 a shift to lower melting temperature, when the pH is increased, is to be expected as usual in the case of negatively charged lipids (36).

Effect of temperature on KcsA conductance

After having established the thermodynamics of our lipid mixtures we performed temperature-dependent single channel conductance measurements of KcsA incorporated in varying molar mixtures of POPE/POPG (3:1, 1:1, 0:1). Traces of the KcsA unitary current as a function of temperature in an asymmetric pH configuration using a virtually solvent-free POPE/POPG 3:1 lipid bilayer are reported in Fig. 2 *a*. Fig. 2 *b* shows KcsA conductance at two holding potentials (50 mV and 75 mV) in a larger temperature range. The two lines represent linear fits to the conductance-versus-temperature data in the higher temperature monotonic region of the graph (from 22°C to 28°C). From our data, it follows that the conductance of the channel is nonmonotonic with temperature. Indeed, upon cooling, at a temperature of 22°C, an increase of the conductance was observed. Upon further decreasing the temperature, a maximum in the conductance was reached, followed by a further decrease. The same behavior was observed for both holding potentials. In the case in which both chambers are set at pH 3, we obtained the same behavior (see Fig. S4 in the Supporting Material).

For a POPE/POPG 1:1 lipid composition, KcsA conductance initially decreased but at 19°C, it started to increase. Interestingly, a monotonic decrease was obtained all over the investigated temperature range for a pure POPG bilayer (Fig. 1 *c*). Fig. 1 *c* also highlights how KcsA conductance depends on the lipid composition of the bilayer; specifically, it increases with the POPG fraction ((31), but see also Fig. S3). To further analyze the anomalous behavior of the conductance, we report the channel conductance versus temperature, after subtracting the linear trend observed for temperatures above 22°C and 19°C for the 3:1 and 1:1 mixtures, respectively (Fig. 1 *d*). Comparing these trends with the corresponding excess heat capacities obtained during downscans at pH 3 (both systematically shifted by −1.5°C), we found a surprising correlation between the variations in heat capacity and ion conductance for both lipid mixtures. Comparing the two mixtures, POPE/POPG

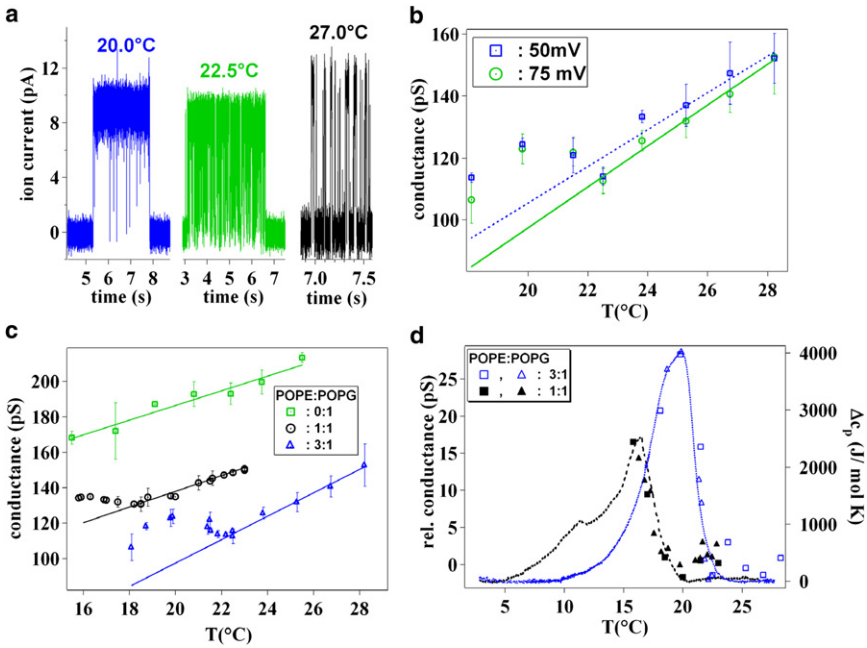

FIGURE 2 Effect of temperature on KcsA conductance. (*a*) Examples of traces of the current for KcsA in POPE/POPG 3:1 at three different temperatures: 27.0°C, 22.5°C, and 20.0°C. Holding potential: 75 mV. (*b*) Plot of the conductance of KcsA reconstituted in POPE/POPG 3:1 as a function of temperature for two holding potentials (□, 50 mV and ○, 75 mV). The two lines are the linear fits to the experimental data in the regions of monotonic behavior of the channel conductance (from 22.5°C to 28.5°C: —, 50 mV; —, 75 mV). Ion conductance changed linearly in a temperature region between 28.5°C and 22.5°C, but upon further cooling, at a temperature of ~22.0°C a trend inversion appeared. (*c*) Temperature-dependent ion conductance of KcsA in BLMs of different POPE/POPG compositions at a holding potential of 75 mV. (*Solid lines*) Respective linear fits in the high temperature region. A nonmonotonic behavior is observed for the two POPE/POPG mixtures (○, 3:1; △, 1:1), but a pure linear trend is found for POPG (□). The trend inversion happened at a lower temperature when KcsA was reconstituted in POPE/POPG 1:1 than in 3:1, accordingly to the shift of the phase transition region for the two lipid compositions. In panels *c* and *d*, the data are given as mean values together with the standard deviation. (*d*) Superposition of the downscan DSC traces at pH 3 (shifted by −1.5°C) for the POPE/POPG 3:1 (—) and 1:1 (—) lipid bilayers with channel conductance at a holding potential of 75 mV after subtraction of the linear fits obtained outside the lipid phase transition. The trend was extended into the transition region. Data points were taken at constant temperature (□, 3:1; ■, 1:1) or during the temperature change (△, 3:1; ▲, 1:1). The changes in ion conductance took place proportionally to the variation of the system's specific heat capacity.

3:1 and 1:1, one has to point out that the anomalous behavior in the ion channel conductance is modulated by the lipid composition used in accordance to the expected changes in the phase transition temperature.

Most important, the linear relationship between KcsA single channel conductance and temperature in a pure POPG bilayer is consistent with the absence of a lipid phase transition in the investigated temperature range. In the case of POPE/POPG 3:1, the KcsA conductance, after reaching a maximum, starts to decrease upon reducing temperature. Instabilities, due to the growth of solid ordered domains, prevented us from performing measurements at temperatures much lower than that at which ion conductance reached its maximum.

It is worthwhile discussing the shift with respect to the DSC traces we performed to compare the thermodynamic behavior of the lipid bilayer with single channel functional behavior. Even if lipid bilayers prepared by the Montal-Muller technique are considered solvent free bilayers, possible residual organic solvent used to assemble the spanning membrane can remain inside the bilayer. In our case, residual hexadecane could affect the thermodynamics and the physical properties of the system, e.g., by changing the packing order of the lipid acyl chains and the lateral pressure profile. Ideally, the characterization of the thermodynamic phase of a membrane and the functional characterization of membrane proteins should be done on the same physical system (27) to compare the data without any correction.

By performing DSC experiments, we established that, preparing small unilamellar vesicles in the presence of 10% hexadecane, the phase transition region shifted by 0.5°C to lower temperature with respect to the pure lipid bilayers. Performing a downscan of the temperature, we observed a strong decrease of the unit area capacitance in the same temperature region at which the trend inversion of the channel's functional properties occurred (see Fig. S1), whereas the unit area capacitance was almost constant outside this temperature region. The behavior of the bilayer capacitance could be considered a strong evidence for the phase transition (37), independently of the knowledge of the exact reason for the shift in the phase transition temperature. In particular, a shift of 1.5°C to lower temperatures of the DSC trace allows aligning the start of the capacitance decrease with the rising of the excess heat capacity. All these observations make us confident that a shift of 1.5° to lower temperature for the DSC traces permits us to overlap the single channel conductance properties to thermodynamic properties of the lipid bilayer hosting the channel.

Many physical properties of the lipid bilayer change abruptly in the proximity of the main phase transition. These also include the surface charge density in a lipid bilayer containing charged lipid molecules. The surface charge density increases in the solid-ordered phase due to the reduced area per molecule. This charge density may, in principle, have a role in the enhanced channel conductance because it can alter the local effective concentration of K^+ near the mouth

of the channel. The effect of the lipid bilayer surface potential on channel conductance has been thoroughly studied (38–40).

In general, the lipid bilayer surface potential is screened by ions in the solution. Thus, the effective surface potential experienced at the mouth of the ion conducting pore is attenuated in the presence of ions in solution. For example, the Debye length, which characterizes the exponential decay of the potential in solution, in 100 mM KCl is 9.6 Å, meaning that the potential at the mouth of the pore for KcsA would be only 6% of the lipid surface potential (40). Marius et al. (31) found a small effect of the surface potential on the differences between KcsA conductances in different bilayer compositions. Furthermore, it has been demonstrated that surface active agents are able to affect the unitary ion channel conductance without involving an electrostatic variation of the bilayer (27). Thus, even if the electrostatic effect may have a role, it does not rule out a possible effect of the lipid bilayer physical properties on the channel behavior. For example, the mechanical properties of a bilayer are affected by ionic strength due to the possible influences on the phospholipid headgroup interactions (41,42). Probably, here a concurrent effect of different mechanisms could be responsible for the channel conductance behavior.

It has been demonstrated that, by changing the acyl chain length of the bilayer hosting the KcsA channel, the tilt angles of the transmembrane helices of KcsA vary along with the hydrophobic thickness of the lipid bilayer (43). This evidence points to a relevant role of channel elasticity in modulating its conductance by bilayer-influenced conformational states. In such a framework, the gating transition involves a variation of the channel conformation at the lipid/protein interface. Thus, the mechanical properties of the lipid bilayer could exert a sort of fine-tuning of the protein conformation, which could alter the free energy variation for an ion passing the filter. Furthermore, small variations in the radius of the KcsA inner pore can produce drastic changes in channel conductance (44). However, specific interactions between KcsA and anionic lipids such as POPG have also been considered (31). To better investigate the reasons for the observed conductance variation, we studied the kinetic features of the channel activity as a function of temperature.

Effect of temperature on KcsA dwell times

KcsA activity is modulated by pH variations at the intracellular compartment, where an acidic pH increases channel open probability (22,23,45–47). Upon opening, KcsA undergoes a further conformational change in which a second gate inactivates the channel (24,45,48). The molecular determinants of both pH sensitivity and inactivation have been elucidated. In steady-state measurements, the dominant gating mechanism is usually attributed to the transition from an inactivated state to an open and conductive state. Consequently, the low open probability of KcsA has been interpreted based on the recovery mechanism from inactivation. Another important aspect of KcsA gating is the presence of a weak voltage dependence even if the channel does not exhibit an evident voltage-sensing domain (49).

A typical single-channel trace is characterized by bursts of activity separated by long closure periods. Intraburst activity is characterized by fast fluctuations of the channel between a conductive and nonconductive state. It has been shown that intraburst activity can involve different modes of activity even under apparently identical experimental conditions. In fact, the kinetic behavior of KcsA features a combination of three distinct modes of channels activity, the low opening probability, high opening probability, and the flickering mode, which appear randomly from patch to patch (50).

In Fig. 3 *a*, we show representative ion current traces of KcsA in POPE/POPG 3:1 at the two temperatures of 27.0°C and 20.0°C. At a temperature of 20°C, we found a maximum for the KcsA conductance in this lipid mixture (see Fig. 2 *d*). Comparing the traces in Fig. 3 *a*, it becomes immediately clear that the KcsA behavior is affected by the temperature as far as characteristic times are considered. We calculated the lifetime distributions at varying temperatures for both the open and closed states.

The results are reported for four different temperatures in Fig. 3, *b* and *c*. The open time distributions, considering exponential components, always show two characteristic times which we define as the longer and shorter opening times. In Fig. 3 *d*, the longer and shorter opening times are reported as a function of temperature along with the downscan DSC trace at pH 3 for the same lipid mixture used in the BLM experiment. Although both times do not change appreciably with temperature above the lipid phase transition region, once the lipid bilayer enters the phase transition, both times increase attaining a maximum along with the excess heat capacity of the bilayer, and then decrease upon further lowering the temperature. In the phase transition region, the open time distribution shifts toward longer durations (51).

The presence of two characteristic open times can be explained by a switching of the channel between different burst modes or by the presence of more than one channel (50). Independently of the interpretation, both times follow the same trend as the excess heat capacity of the lipid bilayer phase transition. The closed time distribution for KcsA (Fig. 3 *c*) is described by one characteristic time which decreases at the lipid phase transition (Fig. 3 *e*) and increases again once the maximum in the excess heat capacity is attained. The open times are more affected by temperature than the closed ones. The longest time observed in the distribution of the closed times can be ascribed to the interburst interval. The same general trend with a slowing down in the transition region that reaches a minimum at the transition midpoint was obtained using the POPE/POPG 1:1 mixture.

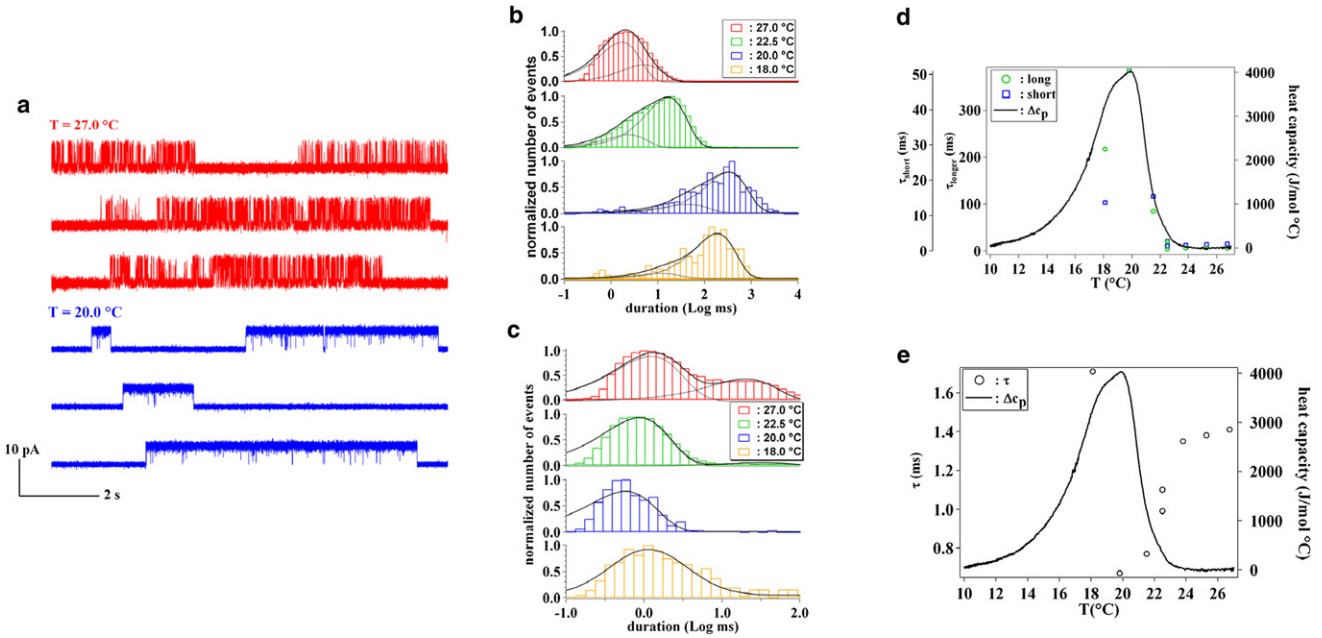

FIGURE 3 KcsA dwell times as a function of temperature at a holding potential of 50mV. (*a*) Examples of ion current traces at temperatures of 27.0°C and 22.0°C in a POPE/POPG 3:1 lipid mixture. Channels are open for longer times at the temperature of 20.0°C where the ion conductance presents a maximum. (*b* and *c*) Dwell-time histograms for the open (*b*) and closed (*c*) states, for KcsA reconstituted into planar bilayers of POPE/POPG 3:1. The open dwell-time and closed dwell-time distributions were fitted with exponential components (⋯) resulting in the overall fit (—). (*d*) Variation of the characteristic open (longer time, ○; slower time, □) and (*e*) closed times (○) with temperature compared to the downscan DSC trace at pH 3 (—, shifted by −1.5°C) of the corresponding lipid bilayer mixture. Open times show the same trend as the specific heat capacity. Closed times present a minimum at the temperature corresponding to the maximum of the excess heat capacity and open times.

Effect of temperature on KcsA normalized open probability

The third functional parameter which is revealed by traces of single channel conductance is the normalized open probability. Fig. 4, *a* and *b*, show the normalized open channel probability versus temperature in the case of POPE/POPG 1:1 and POPE/POPG 3:1 lipid mixtures, assuming a constant number of active channels. At a temperature corresponding to the onset of the lipid phase transition for the used lipid mixture, the normalized open probability also showed a trend inversion. Initially it decreased when lowering the temperature in the region above the lipid phase transition. At 19°C, which corresponds to the onset of the phase coexistence region for the 1:1 lipid mixture, it started increasing until it reached a maximum and then decreased again.

Most of the effect on the normalized open probability is due to a decrease in the closing rates, as it can be deduced by the temperature dependence of the open and closed dwell times. The behavior of open and closed times supports the interpretation of the obtained results in terms of a variation of the normalized open probability rather than a variation in the number of active channels. Fig. 4 *b* shows the normalized open probability for the POPE/POPG 3:1 mixture. In this case, the trend inversion for the open probability occurred at a temperature of 22°C, along with entering the lipid phase transition. The observed behavior for the normalized open probability in both cases points again to a strong connection between the thermodynamics of the lipid membrane and the functioning of the channel.

DISCUSSION

Variations in temperature can affect many biological processes. In the case of proteins in lipid bilayers, temperature can affect both the properties of the lipid ensemble and the conformational transitions of the proteins which underlie their activity. There are several well-documented

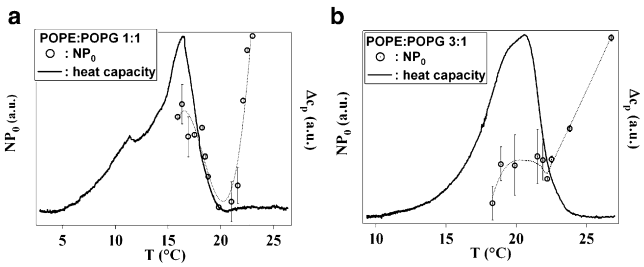

FIGURE 4 Normalized open probability for KcsA in lipid bilayers of different composition compared with the respective downscan DSC analysis at pH 3 (shifted by −1.5°C). (*a*) POPE/POPG 1:1; (*b*) POPE/POPG 3:1. The normalized open probability NP_0 (○, given as a mean together with its standard deviation) in arbitrary units referring to the right ordinate and the specific heat capacity (—) in arbitrary units referring to the left ordinate are reported. In both cases, the open probability had a trend inversion when the system entered the phase transition region.

examples of how the activity of membrane-bound proteins can be modulated by factors affecting the physical properties of the lipid bilayer. These factors include the lipid composition, the lateral pressure profile, the temperature, the curvature, and the thickness of the bilayer (39,52,53). Lipid composition can affect ion channel conductance in different ways: causing specific interactions between lipids and ion channels, altering the surface charge of the lipid bilayer, and modifying lipid bilayer physical properties.

The physical properties of the lipid bilayer can affect the energetic cost of protein conformational changes and can perform a fine-tuning of protein conformation. In the particular case of ion channels, different protein conformations may be associated with rate-determining barriers to ion movements influencing the observed conductance of the channels. Activity of KcsA is strictly connected with its inactivation state. Indeed, KcsA is thought to reside mainly in a long-lived inactivated state with an overall low open probability. The E71A mutant is able to prevent the transition to this inactivated state by removing the Glu^{71}-Asp^{80} interaction.

The intraburst activity is related to the equilibrium between the open-conductive state and an inactivated state. An effect of the lipid phase transition on the intraburst activity where the transition to the inactivated state involves structural rearrangements in the selectivity filter is not immediately intuitive. In fact, this conformational transition seems not to involve the protein/lipid boundary. However, the variation of the channel unitary conductance in the phase transition region supports the idea that the conformation of open KcsA in this region is different from the conformation outside the transition. It is possible that the new conformation alters the rate of transition to/from the inactivated state.

It should be noted that by inducing a phase transition in a POPE/POPG-supported lipid bilayer containing KcsA molecules, these partition preferentially in the vicinity of the domain boundaries and in the liquid-disordered phase of the bilayer (53) (see also Fig. S2). The domain boundaries are characterized by strong local fluctuations (54) and it is expected from thermodynamic considerations that the liquid-disordered regions are richer in POPG with respect to the solid-ordered ones. Thus, KcsA may experience an effective increase in POPG concentration. This phenomenon could also influence the channel conductance in the lipid bilayer via specific lipid/protein interactions. Indeed, it has already been demonstrated that an increase of the POPG content of lipid bilayers induces an increase in KcsA conductance and open probability (31) (see Fig. 2 *c* and Fig. S3).

The sorting of membrane proteins to specific lipid domains with a consequent modification of their function recalls the case of lipid rafts, where the presence of specific lipids promotes the formation of a liquid-ordered phase enriched in cholesterol and sphingolipids. However, two considerations are in favor of an interpretation of the observed variation in functionality not based exclusively on a lipid-specific effect. The first consideration refers to the observed decrease of the KcsA conductance after having reached a maximum inside the transition region. This decrease occurs while the POPG enrichment of the liquid-disordered domains is still going on. The second consideration is connected to a quantitative analysis of the dwell times. We observed a 40–50-fold increase of the dwell times in the POPE/POPG mixtures when the system entered the lipid phase transition region. The longest opening time at a holding potential of 50 mV was 380 ms. This value is significantly higher than the dwell times determined for KcsA in a pure POPG bilayer at the same temperature (see Fig. S5).

These findings can be readily explained by considering the changes in the lipid bilayer's physical state near the phase transition. There, the bilayer reaches a maximum compressibility along with heat capacity (8,42), thus facilitating the protein conformational changes. In addition, it should be mentioned that the associated timescales of the bilayer physical properties are proportional to the bilayer excess heat capacity (9,10). Moreover, the comparison between the dwell times in the case of KcsA in a pure POPG bilayer and in a POPE/POPG 3:1 bilayer at a temperature in which the latter membrane is in the phase transition region allows disregarding the lipid surface charge density variation as the main cause of the observed behavior.

CONCLUSIONS

In conclusion, we have reported that the activity (conductance, dwell times, normalized open probability) of KcsA is finely tuned by the physical state of the lipid bilayer. Here, we studied the liquid-disordered to solid-ordered transition, but it should be possible to extend the same physical concepts to other lipid transitions involving different phases. These experiments prompt further attention to the regulation of membrane protein activity by the lipid environment. Indeed, many of the temperature-induced variations in a lipid bilayer can be equally induced by changes in other parameters such as lipid composition (i.e., lipid synthesis), ionic strength, pH, or by the presence of amphiphilic drugs (27).

SUPPORTING MATERIAL

Five figures and supporting methods are available at http://www.biophysj.org/biophysj/supplemental/S0006-3495(10)01330-5.

KcsA clones were a kind gift of C. Miller. The authors thank C. Miller and A. G. Lee for their critical reading and very useful comments on the manuscript. The authors are indebted to M. F. Schneider and C. Westerhausen for performing DSC measurements on POPE/POPG 1:1 and to M. L. Caiazzo for assistance in protein expression, purification, and reconstitution. The authors declare they have no competing interests.

Partial financial support by Italian MIUR FIRB project No. RBPR05JH2P is acknowledged.

REFERENCES

1. Escribá, P. V., J. M. González-Ros, …, G. Barceló-Coblijn. 2008. Membranes: a meeting point for lipids, proteins and therapies. *J. Cell. Mol. Med.* 12:829–875.
2. Zimmerberg, J., and K. Gawrisch. 2006. The physical chemistry of biological membranes. *Nat. Chem. Biol.* 2:564–567.
3. Lee, A. G. 2004. How lipids affect the activities of integral membrane proteins. *Biochim. Biophys. Acta.* 1666:62–87.
4. Marsh, D. 2008. Protein modulation of lipids, and vice-versa, in membranes. *Biochim. Biophys. Acta.* 1778:1545–1575.
5. McIntosh, T. J., and S. A. Simon. 2006. Roles of bilayer material properties in function and distribution of membrane proteins. *Annu. Rev. Biophys. Biomol. Struct.* 35:177–198.
6. Schmidt, D., and R. MacKinnon. 2008. Voltage-dependent K^+ channel gating and voltage sensor toxin sensitivity depend on the mechanical state of the lipid membrane. *Proc. Natl. Acad. Sci. USA.* 105:19276–19281.
7. Lundbaek, J. A., S. A. Collingwood, …, O. S. Andersen. 2010. Lipid bilayer regulation of membrane protein function: gramicidin channels as molecular force probes. *J. R. Soc. Interface.* 7:373–395.
8. Heimburg, T. 1998. Mechanical aspects of membrane thermodynamics. Estimation of the mechanical properties of lipid membranes close to the chain melting transition from calorimetry. *Biochim. Biophys. Acta.* 1415:147–162.
9. Grabitz, P., V. P. Ivanova, and T. Heimburg. 2002. Relaxation kinetics of lipid membranes and its relation to the heat capacity. *Biophys. J.* 82:299–309.
10. Seeger, H. M., M. L. Gudmundsson, and T. Heimburg. 2007. How anesthetics, neurotransmitters, and antibiotics influence the relaxation processes in lipid membranes. *J. Phys. Chem. B.* 111:13858–13866.
11. Ebel, H., P. Grabitz, and T. Heimburg. 2001. Enthalpy and volume changes in lipid membranes. I. The proportionality of heat and volume changes in the lipid melting transition and its implication for the elastic constants. *J. Phys. Chem. B.* 105:7353–7360.
12. Silvius, J. R., and R. N. McElhaney. 1980. Membrane lipid physical state and modulation of the Na^+,Mg^{2+}-ATPase activity in *Acholeplasma laidlawii B*. *Proc. Natl. Acad. Sci. USA.* 77:1255–1259.
13. Trepat, X., L. H. Deng, …, J. J. Fredberg. 2007. Universal physical responses to stretch in the living cell. *Nature.* 447:592–595.
14. Veatch, S. L., P. Cicuta, …, B. Baird. 2008. Critical fluctuations in plasma membrane vesicles. *ACS Chem. Biol.* 3:287–293.
15. Hoffmann, H. M., and V. E. Dionne. 1983. Temperature dependence of ion permeation at the endplate channel. *J. Gen. Physiol.* 81:687–703.
16. Pahapill, P. A., and L. C. Schlichter. 1990. Modulation of potassium channels in human T lymphocytes: effects of temperature. *J. Physiol.* 422:103–126.
17. Schwarz, W. 1979. Temperature experiments on nerve and muscle membranes of frogs. Indications for a phase transition. *Pflugers Arch.* 382:27–34.
18. Awayda, M. S., W. J. Shao, …, W. G. Hill. 2004. ENaC-membrane interactions: regulation of channel activity by membrane order. *J. Gen. Physiol.* 123:709–727.
19. Fischbach, G. D., and Y. Lass. 1978. A transition temperature for acetylcholine channel conductance in chick myoballs. *J. Physiol.* 280:527–536.
20. Bennetts, B., M. L. Roberts, …, G. Y. Rychkov. 2001. Temperature dependence of human muscle ClC-1 chloride channel. *J. Physiol.* 535:83–93.
21. Thompson, A. N., D. J. Posson, …, C. M. Nimigean. 2008. Molecular mechanism of pH sensing in KcsA potassium channels. *Proc. Natl. Acad. Sci. USA.* 105:6900–6905.
22. Cuello, L. G., J. G. Romero, …, E. Perozo. 1998. pH-dependent gating in the *Streptomyces lividans* K^+ channel. *Biochemistry.* 37:3229–3236.
23. Heginbotham, L., M. LeMasurier, …, C. Miller. 1999. Single *Streptomyces lividans* K^+ channels: functional asymmetries and sidedness of proton activation. *J. Gen. Physiol.* 114:551–560.
24. Gao, L. Z., X. Q. Mi, …, Z. Fan. 2005. Activation-coupled inactivation in the bacterial potassium channel KcsA. *Proc. Natl. Acad. Sci. USA.* 102:17630–17635.
25. Doyle, D. A., J. Morais Cabral, …, R. MacKinnon. 1998. The structure of the potassium channel: molecular basis of K^+ conduction and selectivity. *Science.* 280:69–77.
26. Uysal, S., V. Vásquez, …, A. Kossiakoff. 2009. Crystal structure of full-length KcsA in its closed conformation. *Proc. Natl. Acad. Sci. USA.* 106:6644–6649.
27. Finol-Urdaneta, R. K., J. R. McArthur, …, C. E. Morris. 2010. Modulation of KvAP unitary conductance and gating by 1-alkanols and other surface active agents. *Biophys. J.* 98:762–772.
28. Hirano, M., Y. Takeuchi, …, T. Ide. 2010. Rearrangements in the KcsA cytoplasmic domain underlie its gating. *J. Biol. Chem.* 285:3777–3783.
29. LeMasurier, M., L. Heginbotham, and C. Miller. 2001. KcsA: it's a potassium channel. *J. Gen. Physiol.* 118:303–314.
30. Schmidt, D., Q. X. Jiang, and R. MacKinnon. 2006. Phospholipids and the origin of cationic gating charges in voltage sensors. *Nature.* 444:775–779.
31. Marius, P., M. Zagnoni, …, A. G. Lee. 2008. Binding of anionic lipids to at least three nonannular sites on the potassium channel KcsA is required for channel opening. *Biophys. J.* 94:1689–1698.
32. Montal, M., and P. Mueller. 1972. Formation of bimolecular membranes from lipid monolayers and a study of their electrical properties. *Proc. Natl. Acad. Sci. USA.* 69:3561–3566.
33. Qin, F., A. Auerbach, and F. Sachs. 1996. Estimating single-channel kinetic parameters from idealized patch-clamp data containing missed events. *Biophys. J.* 70:264–280.
34. Qin, F. 2004. Restoration of single-channel currents using the segmental k-means method based on hidden Markov modeling. *Biophys. J.* 86:1488–1501.
35. Pozo Navas, B., K. Lohner, …, G. Pabst. 2005. Composition dependence of vesicle morphology and mixing properties in a bacterial model membrane system. *Biochim. Biophys. Acta.* 1716:40–48.
36. Garidel, P., and A. Blume. 2000. Miscibility of phosphatidylethanolamine-phosphatidylglycerol mixtures as a function of pH and acyl chain length. *Eur. Biophys. J.* 28:629–638.
37. Boheim, G., W. Hanke, and H. Eibl. 1980. Lipid phase transition in planar bilayer membrane and its effect on carrier- and pore-mediated ion transport. *Proc. Natl. Acad. Sci. USA.* 77:3403–3407.
38. Bell, J. E., and C. Miller. 1984. Effects of phospholipid surface charge on ion conduction in the K^+ channel of sarcoplasmic reticulum. *Biophys. J.* 45:279–287.
39. Turnheim, K., J. Gruber, …, V. Ruiz-Gutiérrez. 1999. Membrane phospholipid composition affects function of potassium channels from rabbit colon epithelium. *Am. J. Physiol.* 277:C83–C90.
40. Park, J. B., H. J. Kim, …, E. Moczydlowski. 2003. Effect of phosphatidylserine on unitary conductance and Ba^{2+} block of the BK Ca^{2+}-activated K^+ channel: re-examination of the surface charge hypothesis. *J. Gen. Physiol.* 121:375–397.
41. Böckmann, R. A., A. Hac, …, H. Grubmüller. 2003. Effect of sodium chloride on a lipid bilayer. *Biophys. J.* 85:1647–1655.
42. Garcia-Manyes, S., G. Oncins, and F. Sanz. 2005. Effect of ion-binding and chemical phospholipid structure on the nanomechanics of lipid bilayers studied by force spectroscopy. *Biophys. J.* 89:1812–1826.
43. Williamson, I. M., S. J. Alvis, …, A. G. Lee. 2003. The potassium channel KcsA and its interaction with the lipid bilayer. *Cell. Mol. Life Sci.* 60:1581–1590.
44. Chung, S. H., T. W. Allen, and S. Kuyucak. 2002. Modeling diverse range of potassium channels with Brownian dynamics. *Biophys. J.* 83:263–277.

45. Perozo, E., D. M. Cortes, and L. G. Cuello. 1999. Structural rearrangements underlying K^+-channel activation gating. *Science.* 285:73–78.

46. Liu, Y. S., P. Sompornpisut, and E. Perozo. 2001. Structure of the KcsA channel intracellular gate in the open state. *Nat. Struct. Biol.* 8: 883–887.

47. Jiang, Y. X., A. Lee, …, R. MacKinnon. 2002. The open pore conformation of potassium channels. *Nature.* 417:523–526.

48. Cordero-Morales, J. F., L. G. Cuello, …, E. Perozo. 2006. Molecular determinants of gating at the potassium-channel selectivity filter. *Nat. Struct. Mol. Biol.* 13:311–318.

49. Cordero-Morales, J. F., L. G. Cuello, and E. Perozo. 2006. Voltage-dependent gating at the KcsA selectivity filter. *Nat. Struct. Mol. Biol.* 13:319–322.

50. Chakrapani, S., J. F. Cordero-Morales, and E. Perozo. 2007. A quantitative description of KcsA gating II: single-channel currents. *J. Gen. Physiol.* 130:479–496.

51. R. Antolini, editor. Transport in Biomembranes, Model Systems and Reconstitution. Raven Press, New York.

52. Lundbaek, J. A., and O. S. Andersen. 1994. Lysophospholipids modulate channel function by altering the mechanical properties of lipid bilayers. *J. Gen. Physiol.* 104:645–673.

53. Seeger, H. M., C. A. Bortolotti, …, P. Facci. 2009. Phase-transition-induced protein redistribution in lipid bilayers. *J. Phys. Chem. B.* 113:16654–16659.

54. Seeger, H. M., M. Fidorra, and T. Heimburg. 2004. Domain size and fluctuations at domain interfaces in lipid mixtures. *Macromol. Symp.* 219:85–96.